Enhanced mineralization of bisphenol A by Electric Arc Furnace Slag: Catalytic Ozonation

L.A. Fasce , F. Bocero , C.P. Ramos , N.S. Inchaurrondo

PII: S2666-8211(23)00133-3
DOI: https://doi.org/10.1016/j.ceja.2023.100576
Reference: CEJA 100576

To appear in: *Chemical Engineering Journal Advances*

Received date: 17 September 2023
Revised date: 7 November 2023
Accepted date: 23 November 2023

Please cite this article as: L.A. Fasce , F. Bocero , C.P. Ramos , N.S. Inchaurrondo , Enhanced mineralization of bisphenol A by Electric Arc Furnace Slag: Catalytic Ozonation, *Chemical Engineering Journal Advances* (2023), doi: https://doi.org/10.1016/j.ceja.2023.100576

Enhanced mineralization of bisphenol A by Electric Arc Furnace Slag: Catalytic Ozonation

Fasce, L.A.[1,2], Bocero, F.[1], Ramos. C.P. [3,4], Inchaurrondo, N.S. [1*]

[1] *División Catalizadores y Superficies, INTEMA, Av. Colón 10850, Mar del Plata, Argentina.*
[2] *Departamento de Ingeniería Química y Alimentos, Facultad de Ingeniería, UNMdP, Av. J. B. Justo 4302, Mar del Plata, Argentina.*
[3] *Departamento de Física de la Materia Condensada, GIyA-CAC-CNEA, Av. Gral. Paz 1499 San Martín, Buenos Aires, Argentina*
[4] *Instituto de Nanociencia y Nanotecnología (INN), CNEA-CONICET, Av. Gral. Paz 1499, San Martín, Buenos Aires, Argentina.*

ninchaurrondo@gmail.com

Graphical Abstract

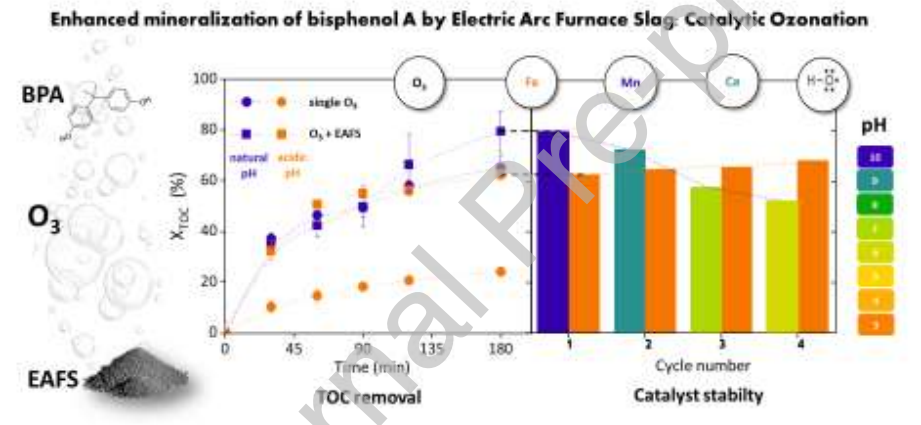

Highlights

- Bisphenol A can be effectively mineralized by the EAFS enhanced ozonation reaction.
- EAFS presents a composition rich in Fe, Ca oxides.
- Outstanding mineralization levels (60-80 %) over a broad pH range (3-10).
- Oxidation occurs through a combination of heterogeneous/homogeneous mechanisms.
- EAFS showed high activity and reasonable stability at a reduced cost.

Abstract:
The catalytic ozonation of bisphenol A (BPA) was performed using an industrial solid waste as catalyst: electric arc furnace slag (EAFS). The characterization of the catalyst (SEM/EDS, XRD, surface area, pH_{PZC} and Mössbauer spectroscopy) showed low surface area, alkaline nature and a composition rich in Fe, Ca, Si, C oxides, with minor content of Mg, Mn and Al. Ozonation experiments were carried out in a semi-batch reactor at room temperature at different initial pH conditions: from alkaline (natural pH 10.5) to acidic (controlled pH 3) aqueous media. Catalytic ozonation experiments showed complete BPA removal and remarkable total organic carbon conversions (62-80%) over the broad pH range explored. The highest mineralization levels were obtained under basic pH, which was attributed to the generation of hydroxyl radical given by the presence of OH^- and precipitation reactions of intermediates promoted by Ca oxides. Under acidic conditions the presence of EAFS notoriously enhanced BPA mineralization compared to single ozonation, due to the activity of leached species. The stability of the material was tested in 4 ozonation cycles. EAFS activity was mostly sustained under acidic conditions while a reduction was observed under uncontrolled pH condition, which was associated with a marked pH decrease. However, the residual activity still allowed complete BPA degradation and high mineralization levels (> 50 %). EAFS is a low-cost material that exhibits high activity and reasonable stability in catalytic ozonation of BPA. The valorization of this waste constitutes a technological alternative that could benefit both metallurgical and water treatment plants.

Keywords: electric arc furnace slag, ozonation, catalysis, bisphenol A, emerging pollutants.

1. Introduction

Emerging pollutants are previously unknown or unrecognized pollutants, composed of products used in large quantities in everyday life, such as human and veterinary pharmaceuticals, personal care products, surfactants and surfactants' residues, plasticizers, and different industrial additives [1]. One of the main characteristics of these contaminants is that they do not need to be persistent in the environment to cause negative effects since their high transformation/removal rates can be compensated by their continuous introduction into the environment [1]. Within this group, bisphenol A (BPA; 2, 2-bis (4-hydroxyphenyl) propane) has shown endocrine-disruption in living beings and despite the mounting evidence around this, its demand still presents an upward trend [2,3]. BPA is used in large volumes to produce polycarbonate plastics and epoxy resin linings that are applied in the manufacture of a wide range of consumer goods such as metal-based food and beverages cans, water supply pipes and dispensers, toys, medical tubing, power tools, baby bottles, and furniture [2]. BPA migration from BPA-based products into the aquatic environment can be a source of contamination in low concentrations and higher values can be found in polycarbonate and epoxy plant wastewaters (around 50 mg/L) [4] or in landfill leachates (up to 17 mg/L) [5].
Untreated urban effluents and effluents from landfill sites and water treatment plants that are not designed to treat this type of substances are among the main sources of this kind of pollutants [1,6]. Since ozone is a powerful oxidant, capable of reacting with many organic and inorganic compounds [7], this study proposes the use of catalytic ozonation for the elimination of BPA. The proposal aims to contribute to the development of viable technologies for the treatment of emerging pollutants.
Ozonation has shown promising results in terms of BPA removal [8,9]. However, achieving complete

mineralization and preventing the formation of harmful by-products can be challenging. Garoma et al. [8] studied the ozonation of BPA and its reaction intermediates, observing that while the process effectively oxidized BPA, the reaction intermediates were more resistant to ozone compared to the parent compound. Further mineralization of BPA required a significantly prolonged ozonation process. To enhance the efficiency of the ozonation process, the use of catalysts has been extensively investigated, driving research studies in the field of materials science and water treatment processes. This work proposes the use of electric arc furnace slag (EAFS) as a catalyst for the ozonation reaction, primarily due to its composition rich in iron oxides, which have proved to be active sites in the ozonation reaction. EAFS is a by-product that consists mainly of silicates and oxides formed during the process of refining the molten steel. The proposal is encouraged by the potential applications of ferrous slag materials in water and wastewater treatments recently highlighted by Sahu et al. [10] and by the benefits for both the metallurgical industry and water treatment plants. Ferrous slags can be used as coagulants, filters, adsorbents, neutralizers/stabilizers, catalysts, additives, and bed materials [10]. Specifically, their utilization helps to minimize the volume of waste material that needs to be disposed, reduces the reliance on expensive chemical reagents used in water purification, and enables the repurposing of unhealthy aquatic resources for other uses, such as human consumption or irrigation.

Promising results regarding the use of steel residues such as EAF slag/dust or basic oxygen furnace slag in the field of Advanced Oxidation Processes for water treatment have been recently reported, with most studies based on Fenton and photo-Fenton reactions [10–15]. However, there are only few references in the use of metal slag wastes as catalysts for ozonation reactions [16,17] and no-one specifically related to BPA degradation. Van et al. [16] employed iron slag wastes, containing FeO, ZnO and SiO_2 for Fenton and ozonation reactions to remove an azo dye. The combination of ozone with the metal slag had a synergistic effect on the dye degradation since the catalyst promoted the decomposition of O_3 and generation of hydroxyl radicals. Hien et al. [17] studied the catalytic ozonation of another dye, Direct Black 22, in the presence of waste metal slags. The presence of Ca and Zn played an important role in the discoloration and mineralization rate through a complex mechanism, much related to the alkaline condition generated by the material, which promoted the formation of radicals. The results drawn by these studies may differ since the composition of waste metal slags could be quite variable, with a usual majority of Fe, Zn, Ca, Si and Mn oxides.

The purpose of the present study is to evaluate the performance of an EAFS sample provided by a local metallurgical company, as a catalyst for the ozonation of a BPA aqueous solution. EAFS composition is characterized in detail and linked to the observed ozonation reaction mechanism and catalyst stability under different pH conditions.

2. Methodology

2.1 Characterization of EAFS

The characteristics of raw and used EAFS samples were determined by different techniques.

Sample morphology and elemental composition were investigated by means of a scanning electron microscope (SEM) Zeiss Sigma 300 complemented with energy dispersive X-ray spectroscopy (EDS).

Powder X-ray Diffraction (XRD) was conducted with a PANalytical X'Pert Pro diffractometer by using CuKα radiation (λ = 1.54056 Å) to derive the presence of different phases from the crystal structure of the samples.

Mössbauer spectra were obtained at room temperature (RT) with a conventional constant acceleration spectrometer in transmission geometry with a ^{57}Co/Rh source, to characterize the iron-bearing components of the samples. Measurements were recorded at 10 mm/s and then fitted using the Normos program developed by Brand [Normos program by R.A. Brand (http:// www. wissel- gmbh. de)]. Isomer shift values (IS) are listed relative to that of α-Fe at RT. The relative proportion of each iron site in a phase structure was estimated assuming that the Mössbauer effect probability was the same for all positions.

Specific surface area was determined by N_2 adsorption/desorption at -196ºC (Micromeritics, model TriStar II 3020) and calculated by means of the Brunauer–Emmett–Teller (BET) theory. Pore-size distribution was assessed from the desorption branch of the nitrogen isotherm employing the BJH method.
The point of zero charge (PZC) was determined by the mass titration method [18]. The measurements were conducted at 25°C in either 25 mL or 100 mL of 0.005 mol/L NaCl aqueous solutions, which were purged with N_2. Portions of the sample were added to stirred aqueous solutions with initial pH = 6. In the case of the 3 points measured in 100 mL suspensions, portions of 0.0014, 0.004 and 0.008 g of the sample were added. For the 25 mL suspensions, portions of 0.005 g were added within the range of 0.005 g to 0.1 g. The suspension´s pH stabilized after 5 hours. As the solid-to-liquid ratio increased, the pH of the system gradually changed until it eventually stabilized at a constant value, which corresponded to the PZC.
A quantitative screening of the leached species under acidic conditions (pH 3, 0.5 g/L of catalyst, 3 h contact, 24°C) was performed by inductively coupled plasma mass spectrometry (ICP-MS, Agilent, ASX-500) to evaluate the risk of leachability of hazardous heavy metals present in the sample composition.

2.2 Oxidation tests

2.2.1. Materials and reagents

BPA (Sigma-Aldrich, 99 %), H_2O_2 (30%w/w, Anedra), HNO_3 (65%w/w, Cicarelli), NaOH (Anedra, 97 %), $Fe(NO_3)_3.9H_2O$ (Anedra, 98.1 %), $Mn(NO_3)_2 \cdot 4H_2O$ (Sigma-Aldrich, 97 %), NaCl (Merck, 99.9 %). Reagents for Fe determination: 1,10 phenantroline (Sidma-Aldrich, > 99.0 %), hydroxylamine hydrochloride (Analyticals Carlo Erba 99 %), HCl (Merk, p. a. min. 37 %). Reagents for BPA determination: NH_4OH (Cicarelli., p. a., 28-30 % v/v), Na_2HPO_4 (Cicarelli, p. a), NaH_2PO_4 (Cicarelli, p. a), potassium ferricyanide (Anedra, 99.4 %), 4-aminoantipyrine (Sigma-Aldrich reagent grade, > 98 %).
EAFS was provided by a local metallurgical company; this material is a fine dust that was used as received (see please Fig. S1 in Supplementary Material (SM) section).

2.2.2. Analytical procedures

BPA concentration was quantified using a colorimetric assay developed for phenolic compounds [19] in a Shimadzu UV-1800 spectrophotometer.
Total organic carbon (TOC) was determined in a TOC analyzer Shimadzu (model TOC-VCPN).
Leached Fe and Mn ions were determined by standard colorimetric tests: 1,10-phenantroline method for Fe(II) and Fe(III) [19] and Hach reagent for Mn (Manganese reagent set LR, PANmethod).
The dissolved ozone concentration was determined according to the indigo method [19].

2.2.3. Ozonation reaction conditions

The BPA solution (20 mg/L) was prepared by dissolving BPA powder in Milli-Q water.
All ozonation reaction tests were performed at RT (23-24ºC) during 3 h in a 1 L semi-batch stirred-tank reactor under vigorous agitation. The ozone was bubbled into the reactor continuously, fed through a porous stainless-steel diffuser with a concentration in the gas phase of 10 mg/L and a gas flow of 700 mL/min. Ozone was generated from pure oxygen with an Enaly KNT24 generator. The ozone concentration in the gas phase was monitored using a BMT64 sensor. The residual ozone was eliminated with a catalyzing cartridge (BMT, Carulite 200). Catalytic ozonation tests were carried out

pouring 0.5 g/L EAFS in the reactor and keeping it in contact with BPA solution for 45 min before starting the ozonation reaction. During the tests, aliquots of reaction media were taken periodically from the reactor and immediately analyzed to determine pH, TOC, BPA, and leached Fe and Mn concentrations.

Several reaction tests were carried out to evaluate EAFS performance as a catalyst for BPA mineralization under different pH conditions, to give insight into the ozonation mechanism and to assess EAFS stability. All performed tests conditions are given in Table 1 and described in what follows.

To investigate potential variations in the reaction mechanism across a wide pH range, single and catalytic ozonation experiments were conducted under both alkaline (tests #1 and #3, Table 1) and acidic (tests #2 and #4, Table 1) conditions. The natural pH of the BPA solution in contact with 0.5 g/L of EAFS is 10.5. Due to the generation of carboxylic acids during the ozonation reaction, the pH gradually tended to decrease, reaching a value of 9.5 after 3 h of reaction. Consequently, the average pH throughout the ozonation reaction in the presence of EAFS was found to be 10. Comparative single ozonation experiments were therefore carried out at a constant pH of 10, which was carefully maintained by adding NaOH (5 mol/L) as required. On the other hand, acidic conditions were expected to result in higher leaching, which could significantly impact the progression of the reaction. Therefore, catalytic, and single ozonation tests were performed at constant pH 3, which was controlled by the addition of 4 mol/L HNO_3.

To analyze the contribution of EAFS leached species, first 0.5 g/L EAFS was kept in contact with BPA solution during 1 h, then EAFS was removed by filtering and the ozonation reaction was carried out using the supernatant liquid as the reaction media (test #5 and #6, Table 1). Catalytic homogeneous tests using Fe (III) and Mn(II) dissolved salts were also carried out for comparison (tests #7 and #8, Table 1), since both cations proved to be active in ozonation reactions according to previous studies [20].

Catalyst reusage experiments were conducted by a series of 4 successive ozonation cycles (test #9 and #10, Table 1). After the first test, EAFS load was left to settle in the reactor and the residual reaction supernatant was collected. Then the catalyst was washed with Milli-Q water and settled again in the reactor. Finally, the water was eliminated, and new BPA solution was incorporated to start the next test of the series. These steps were repeated 3 times.

Complementary single ozonation experiments (tests #11, #12, #13 and #14) were also carried out at intermediate pH conditions to elucidate the influence of pH on BPA mineralization process.

To evaluate the possible adsorption of BPA in EAFS, batch adsorption experiments (tests #15 and #16, Table 1) were executed under the main conditions studied in ozonation reactions (pH 3 and 10). BPA solution (20 mg/L) was contacted with EAFS particles (0.5 g/L) during 3-4 h in a laboratory rotary shaker at room temperature. Then, the supernatant samples were analyzed to determine BPA concentration before and after the test.

Finally, to give insight into the study of the ozonation mechanism under alkaline conditions, a two-step experiment was designed (test #17, Table 1). First, the BPA solution was ozonized at pH 10 for 2 h. Then the ozone was removed by bubbling nitrogen in the solution and the remnant supernatant was employed in adsorption tests with 0.5g/L of EAFS at a pH of 10.5 during 90 min of contact.

3. Results and discussion

3.1. EAFS characterization

The raw EAFS sample showed a low BET surface area of 0.9 m^2/g, with a pore volume of 0.003 cm^3/g and average pore width of 12.2 nm, denoting a nonporous material.

SEM micrographs revealed the presence of very fine particles with heterogeneous shapes and sizes (see please Fig. S2 in SM section). Table 2 displays the elemental weight composition determined via SEM/EDS showing that it is rich in O (41.1 %), Fe (16.2 %), Ca (13.2 %), C (18.9 %), Si (3.7 %), with

minor contents of Mg (2.6 %), Mn (1.8 %) and Al (1.4 %). In addition, it contains traces (below 1 %) of several elements which randomly appeared depending on the analyzed spot, such as Cr (0.6 %), Ti (0.2 %) or Cu (0.1 %).

From the XRD pattern, the higher intensity peak at 42.09° (Fig. 1-a), which is located between the main peaks of pure wustite - FeO - (41.89°) and periclase - MgO - (42.92°), reflects the majority phase, a ferrous oxide called magnesiowustite. Larnite (Ca_2SiO_4), with the characteristic three main peaks at 31.99°, 32.61° and 32.17°, is also detected. Larnite may be the product of the reaction of CaO and SiO_2 during the melting process in the electric arc furnace. A minor contribution of akermanite ($Ca_2MgSi_2O_7$) shows up at 31.20° and 47.50°. Other iron oxides, as hematite (Fe_2O_3), magnetite (Fe_3O_4) and/or maghemite, and some quartz and metallic iron are present as minority phases. A broad peak at low diffraction angle suggests an amorphous or poorly ordered contribution with very fine particles. This could be a consequence of water quenching following melting in the EAFS, resulting in some glass content.

MgO containing additions are used in steelmaking processes to protect refractories. Solid MgO is fully soluble in both FeO and MnO, forming a continuous solid solution [21]; thus magnesiowustite with incorporation of Mn is commonly found in the mineralogical composition of EAF steel slags [22], which explains the presence of Mn in EDS measurements.

Mössbauer spectroscopy gives information about the iron-bearing components of a sample and is very useful in discriminating Fe^{2+} and Fe^{3+} contents of non-stoichiometric minerals. A hyperfine field distribution (hfd) and four doublets were employed to fit the Mössbauer spectrum of the raw slag sample (Fig. S3 in SM section). The obtained hyperfine parameters are listed in Table 3. The hfd is related to the existence of magnetically ordered iron oxides at RT, such as magnetite, maghemite and hematite, and of a scarce content of goethite (ferric iron oxyhydroxide) and metallic iron. The doublets (D1 – D4) are associated to a paramagnetic phase at RT, characteristic of non-stoichiometric magnesiowüstite. Four of them got IS values which represent high spin Fe^{2+} at octahedral sites, due to the range of different symmetries of the Fe^{2+} environments in the structure caused by diverse iron contents and cation vacancy levels; and the other one is related to Fe^{3+} in tetrahedral sites (coordination VI) [23].

All the employed characterization techniques agree, showing that Fe and Ca are the main components of the steel slag.

The pH_{PZC} of the EAFS sample reached a value of 11 (Fig. S4 in SM section). This result is explained by the presence of Ca species in EAFS, which dissolves in water to form $Ca(OH)_2$, making the solution strongly alkaline.

Considering the potential application of EAFS in water-treatment processes, it is crucial to assess the environmental impact of EAFS, especially for the hazardous elements (heavy metals) present in its composition and the possible risk of their leachability [10,24]. The leaching test performed under acidic conditions (pH 3, 0.5 g/L of catalyst, 3 h contact, 24°C) delivered the following composition: Na 0.25 mg/L, Mg 0.68 mg/L, Al 0.15 mg/L, Cu 0.15 mg/L, Ca 14 mg/L, Fe 7.29 mg/L, Ti 0.069 mg/L, V 0.085 mg/L, Cr 0.084 mg/L, Mn 0.81 mg/L, Ni 0.21 mg/L and Zn 0.29 mg/L. The concentration values of these ions do not exceed the maximum admitted for sewage discharge in the Argentinian region (Resolution 79.179 from ex Obras Sanitarias de la Nación, decrees 674/89 and 776/92). This excellent finding is in alignment with previous studies on the leaching behavior of iron slags, with compositions like the one used in this work [10,25]. These studies demonstrated experimentally, by applying several leaching test techniques, that the leaching of hazardous heavy metals is either insignificant or falls below the permitted levels established by the USEPA (United States Environmental Protection Agency) [10,25].

3.2. Ozonation tests

3.2.1. BPA removal

To analyze the adsorption capability of BPA in an EAFS sample, adsorption tests were carried out at both acidic and alkaline conditions (pH 3 and 10). No removal of BPA was observed in the experiments, in agreement with the low surface area of the EAFS.

Complete BPA degradation was observed in all ozonation experiments, and it occurred during the first minutes of reaction. Fig. 2 shows the evolution of BPA conversion found in single ozonation tests at both acidic and alkaline initial pH conditions. Overall, BPA degradation reaction proceeded very fast during the first 10 min of reaction and it was completed at about 20 min. The fast BPA degradation agrees with the low ozone concentration detected in the aqueous phase during the first minutes of reaction, as exemplified in Fig. 2 for acidic conditions. It has to be pointed out that in a test without BPA, we measured the time it takes to saturate Milli-Q water with O_3, under the tested conditions. After only 4 min, the concentration in the aqueous media increased up to 1.8 mg/L average (Fig. S5 in SM section). In the experiments with BPA it takes 30 min to reach that value, which occurs once BPA is removed.

In single ozonation tests, BPA conversion followed a pseudo-first order kinetic rate law as judged by the good regression coefficients obtained ($R^2 > 0.99$) as shown in Fig. 2. The fitted pseudo-first order kinetic constants are $5.2x10^{-3}$ s^{-1} and $2.9x10^{-3}$ s^{-1} for pH 10 and pH 3, respectively. These values are within the range of those reported in literature [26]. The improvement in BPA oxidation rate at alkaline pH can be related to the well-known generation of hydroxyl radicals promoted by the presence of OH^- or to the higher reactivity of ozone towards ionized BPA [7,9,26].

3.2.2. BPA mineralization

3.2.2.1 BPA mineralization by single ozonation tests

The evolution of BPA mineralization in single ozonation reaction tests is shown in Fig. 3 for both pH conditions (pH 3 and 10). Despite BPA was completed degraded at a brief reaction time (Fig. 2), a considerable amount of unreacted TOC remained in the solution even after 3 h of reaction. As expected, pH greatly influenced the degradation process. According to the results shown in Figs. 1 and 2, not only BPA removal but also mineralization is enhanced at basic pH conditions because of the already mentioned generation of •OH species that are less selective than ozone. TOC conversion increased from 24 to 65% by increasing the pH from 3 to 10. Fig. 4 shows the TOC conversion achieved after 3 h in single ozonation experiments carried out in a broad range of pH conditions. The main enhancement in TOC conversion appears to occur around pH 5.5-6 (Fig. 4).

Specific studies have focused on the identification of reaction intermediates generated during BPA ozonation, employing different sophisticated techniques (*i.e.* GC, LC–UV, LC–MS or MS/MS) [8]. Garoma et al. [8] identified catechol, resorcinol, acetone, formaldehyde in a first step and organic acids, acetic, formic, maleic, and oxalic acid, as final reaction products. These intermediates were found to be more resistant to ozone attack, hindering the complete mineralization of the target compound. To address this limitation, in the subsequent sections we investigated the impact of adding EAFS in the mineralization of BPA. Reaction tests were performed under two different pH conditions strategically selected: i) acidic conditions (pH 3) and ii) without pH control that results in pH around 10 due to the alkaline nature of EAFS. Acidic conditions are expected to result in higher active species leaching, which could significantly impact the progression of mineralization while the natural alkaline conditions of EAFS are expected to favor hydroxyl radical formation. Main results are presented in Figs. 5-a) and 5-b) and discussed according to the pH condition explored.

3.2.2.2. BPA mineralization by catalytic ozonation tests at average pH 10

Mineralization results obtained in catalytic ozonation tests at alkaline conditions are shown in Fig. 5-*a*). Single ozonation results at pH 10 are also included for comparison in the graph. The presence of

EAFS enhanced the BPA mineralization rate as well as the mineralization degree achieved at the end of the test. After 3 h of reaction 80% of TOC removal was obtained. As mentioned before, EAFS is alkaline in nature, and it keeps the pH of the BPA solution up to an average of 10. However, the mineralization level obtained in the presence of EAFS resulted higher than that reached in single ozonation tests at pH 10 (65 %). This could be related to synergistic effects linked to the complex composition of the material. According to EDS and XRD characterization results discussed in section 3.1, EAFS presents abundant Ca species. Several studies reported the use of $CaO/Ca(OH)_2$ based materials as catalysts and/or precipitants in the ozonation of organic pollutants such as tetrakis hydroxymethyl phosphonium sulfate [27], sulfonale [28], acid red 18 [29] and high salt organic wastewater [30]. Different mechanisms have been proposed to explain the role of calcium oxides in ozonation reactions. Some studies agreed that calcium oxides dissolve in water to form $Ca(OH)_2$, making the solution strongly alkaline, favoring the generation of •OH [27–29]. Zhou et al. [27] reported that the O_3 molecule may be adsorbed onto the Ca atom on the surface of $Ca(OH)_2$ to form the ozonide of calcium by a terminal atom. Then, H_2O would accelerate the decomposition of calcium ozonide to form O atoms and $^{-}•O_2$, and H_2O would decompose to form •OH. Quan et al. [29] reported that the elimination of CO_3^{2-} ions, a common radical scavenger, as $CaCO_3$, could also enhance the efficiency of the ozonation reaction. Moreover, the presence of Ca^{2+} could promote the precipitation of other molecules, such as oxalic acid, which is a common final reaction intermediate, causing a reduction of the organic carbon content of the treated solution [31,32].

The EAFS catalyst also presents an important amount of Fe species and a minor amount of Mn, as observed by EDS, XRD and Mössbauer spectroscopy analysis. The catalytic properties of Fe or Mn oxides in the ozonation reaction have been mainly attributed to their acidity or basicity character. Both Brönsted and Lewis acid sites are thought to be the catalytic centers on metal oxides, mainly for the adsorption and favorable decomposition of ozone molecules [20]. Different studies have proved that deprotonated ($pH > pH_{PZC}$) or neutral surface hydroxyl groups ($pH = pH_{PZC}$) have a strong reactivity towards ozone [33,34]. Other studies reported higher activity at lower pH values ($pH < pH_{PZC}$) with a mechanism based on surface adsorption and complexation of organic molecules (i.e. oxalic acid) or a mechanism based on the activity of leached species [35,36]. In our case, with the simple addition of EAFS and performing no pH control, the reaction takes place at a pH slightly lower than the pH_{PZC} of the material.

Discriminating the individual roles of the various elements comprising the catalyst in the reaction pathway appear to be extremely challenging. It is reasonable to assume that under this condition (no pH control) the role of Ca species stands out, since alkalinity is key in O_3 decomposition into reactive oxygen species. The improvement in TOC removal by EAFS, beyond the observed in single ozonation at pH 10, may be related to the precipitation of final reaction intermediates, such as oxalic acid, caused by Ca^{2+} ions. However, the participation of Fe and Mn oxides as active phases cannot be discarded.

To evaluate the role of leached species, ozonation experiments using the supernatant as reaction media were carried out. Mineralization evolution results are included in Fig. 5-*a*). A lower mineralization level than that obtained with the catalyst powder was reached with the supernatant. The reaction starts at the natural pH of the supernatant (10.5) and as it evolved, the pH dropped to 9 after 90 min and to 8, at the end of the test. This pH variation could explain the lower activity observed with the supernatant compared to the alkaline test in the presence of EAFS and to single ozonation at constant pH 10.

The results obtained with EAFS in this section aligns with previous studies that have explored the use of materials to enhance the ozonation reaction through the generation of alkaline conditions. For instance, Dong et al. [37] and He et al. [38] investigated the use of natural brucite ($Mg(OH)_2$) or magnesia (MgO); studies involving CaO [27–29] have also been conducted. This background information serves as example of how alkaline-generating materials can contribute to the enhancement of the ozonation process.

The natural alkaline pH originated from contacting EAFS powder with the BPA solution is clearly effective in improving BPA mineralization with respect to the single ozonation, but also the

contribution of leached cations, mainly Ca^{+2}, might be further enhancing TOC removal, in the last hour of reaction.

3.2.2.3. BPA mineralization by catalytic ozonation tests at pH 3

Mineralization results obtained in catalytic ozonation tests at acidic conditions (pH 3) are shown in Fig. 5-*b*). Single ozonation results for the same pH value are also plotted for comparison. At pH 3, the presence of EAFS enhanced the TOC conversion from 24 % (single ozonation) to 63 % (with EAFS powder). Under this pH condition, the incorporation of the catalyst drastically improved TOC removal compared to that obtained in the single ozonation test. As well, the mineralization obtained with the supernatant almost matched the evolution of the ozonation reaction with EAFS powder. Therefore, under acidic conditions the catalyst seems to be acting as a dispenser of effective active species. In the study on catalytic ozonation of organic phosphorous wastewater by CaO [27], Ca did not show any activity at pH 3 or 5. Then, the catalytic effect of EAFS may be mainly attributed to the presence of Fe or Mn leached species, which have been proved to be active in ozonation reactions even at very low concentrations [39–41]. This behavior has also been observed in several heterogeneous catalytic processes. For example, Yang et al. [41] determined the metal leaching from several solid catalysts (copper and silver oxide-based catalysts) and investigated the influence of the leached ions on the mineralization of two model compounds (oxalate and nitrobenzene). The homogeneous catalytic effect was found to be the dominant mechanism for the degradation of the pollutants under the chosen experimental conditions.

3.2.3. EAFS Stability

The effect of EAFS reusage on the mineralization degree of BPA by catalytic ozonation experiments was studied at both pH conditions.

3.2.3.1 EAFS stability under uncontrolled pH conditions

Results of TOC conversion obtained in EAFS stability experiments (test #9, Table 1) are shown in Fig. 6-*a*). It is found that without pH control there is an important loss of activity, especially during the first 3 cycles. The TOC removal descends from 80% in the first cycle to an average of 54% in the third and fourth cycles. To study the cause of EAFS deactivation, the leaching of different species of interest was evaluated, together with the pH of the reaction media. The concentration of leached species and initial and final pH values are presented in Table 4.

Under alkaline conditions, the concentration of leached species of Fe and Mn resulted very low. Therefore, their contribution to BPA mineralization under this pH condition seemed negligible. From cycle to cycle, as the catalyst was reused, the initial pH decreased. This could be related to the loss of $CaO/Ca(OH)_2$ species in the reaction media. Note that the second cycle shows a similar evolution to the single ozonation test at pH 10, which can be explained by a lower contribution of Ca^{2+} as a precipitant. Moreover, the further reduction in activity could be related to the continued loss of alkalinity of the catalytic material. Note that the loss of mineralization with reducing pH condition was also observed in single ozonation experiments (Fig. 4).

The third and fourth cycles elapsed under neutral or slightly acidic pH. Under this condition, the mineralization evolution matches the curve obtained in the single ozonation test with the same pH evolution (pH 7 to 5.5, average pH 6) as shown in Fig. 6-a). Then, it appears that the catalyst is slowly deactivating as it loses its capability to basify the reaction media.

To provide insights into the reaction mechanism under uncontrolled pH conditions, test #17 (Table 1) was designed. At the end of the first step of the experiment (90 min of catalytic ozonation), TOC conversion was 48% while a further increase of 35 ± 6 % was obtained in the adsorption step. The material exhibits a very low surface area, so this TOC removal could be a consequence of the action of

Ca^{2+} as a precipitant of final reaction intermediates, such as oxalic acid. The EDS characterization (Table 2) shows a lower content of Ca in the samples used after four cycles, confirming the idea that the role of Ca species diminishes as the catalyst is reused. This is also confirmed by the other characterization techniques. XRD pattern of the 4 times reused catalyst under uncontrolled pH conditions was evaluated and compared with that corresponding to the raw one, in order to investigate structural changes after the reaction. The crystal phases observed are almost the same to those of the raw slag precursor (Fig. 1-b). However, the procedure improved the crystallinity, and there was a slight rearrangement presumably due to the leaching of active species, such as calcium, during the reaction. This is evidenced by the abrupt decrease in the intensity peaks of larnite and quartz. It is also interesting the occurrence of ankerite ($Ca(Fe,Mg,Mn)(CO_3)_2$). Then, the removal of CO_3^{2-} ions, common radical scavenger, could also favor the reaction.

The corresponding Mössbauer spectrum is quite similar to that of the raw slag sample (Fig. S3 in SM section). A hyperfine field distribution and four doublets were also employed to fit the Mössbauer spectrum (Table 3). The doublets (D1 – D4) are associated to non-stoichiometric magnesiowüstite and the hfd to a minor contribution of magnetite, maghemite, hematite, goethite and metallic iron. The proportion of each one of the sites in magnesiowustite and of the other iron oxides, oxyhydroxide and metallic iron showed a slight change in comparison with the raw EAFS sample spectrum (see Table 3), reinforcing the hypothesis of a low Fe and Mn leaching.

3.2.3.2 EAFS stability under acidic conditions

Results of TOC conversion obtained in EAFS stability experiments at constant pH 3 (test #10, Table 1) are shown in Fig. 6-b). In this case, the concentration of leached Fe and Mn ions is important (see Table 4). There is a decay in activity between the first and second cycle. Then, the activity mostly sustains over the cycles. This could be mostly connected to the lower presence of Mn in the reaction media solution. In the first cycle, a concentration of 0.41 mg/L was measured at the end of the reaction. For the rest of the cycles, the Mn concentration decreased and ranged between 0.06-0.08 mg/L. The presence of Mn is also visible through the purple/pink coloration that the solution acquires as the reaction evolves (see SM Fig. S6).

The role of Mn^{2+} on the catalytic ozonation of organic pollutants has been reported by other authors [42,43]. Ma et al. [43] studied the manganese catalyzed ozonation of atrazine and observed that a relatively low amount of Mn^{2+} (0.3 mg/L) was able to catalyze the decomposition of ozone via intermediate manganese species, generating radical species. Andreozzi et al. [42] studied the use of MnO_2 for the catalytic ozonation of oxalic acid and observed catalytic effect at moderately acidic pH values, since the electrostatic attraction with the protonated surface facilitated the adsorption of oxalic acid. The catalytic effect was based on the formation of a surface manganese-oxalic acid complex to give an intermediate product that was more easily degraded by ozone. Also, the complex formation followed by a "one electron" exchange step, could cause the detachment of the reduced surface center and leaching of Mn. Manganese catalyzed the decomposition of ozone generating hydroxyl radicals and at the same time Mn^{2+} was oxidized by ozone to form higher valent manganese oxide. Depending on the ozone concentration and the presence of reducing compounds (Fe(II), reaction intermediates), insoluble MnO_2 as well as soluble Mn^{2+} or MnO_4^-, recognizable by its pink color, could be obtained [44].

Results of complementary ozonation tests performed by adding 0.1 mg/L Mn or 4.5 mg/L Fe to the BPA solution are also shown in Fig. 6-b. They evidenced the active role of Fe and Mn species in the leachate, showing final mineralization levels of 49 % in the case of Fe and 60 % in the case of Mn. However, it is important to note that these experiments do not accurately replicate the variation in concentration and oxidation state of the leached species throughout the heterogeneous oxidation tests. Specifically, in the case of Mn, it should be noted that a dynamic cycle involving Mn^{2+}, MnO_2, and MnO^{4-} may occur during the ozonation reaction. Furthermore, at the end of each test, a portion of the

manganese species may have precipitated as MnO_2 on the catalyst surface. This phenomenon could potentially explain the long-term stability observed in the EAFS sample over multiple cycles. Additionally, the substantial presence of iron oxides in the solid sample -evidenced in the Mössbauer spectra- ensures a continuous supply of Fe cations, further contributing to the sustained performance of the catalyst.

These results are in tune with the XRD diffraction pattern of the 4 times used catalyst under acidic conditions, which was compared with that of the raw slag and the one for uncontrolled pH to follow the structural changes (Fig. 1-*c*). There was an evident rearrangement due to the leaching of active sites during the reaction. Ankerite occurred but the other calcium compounds as larnite and akermanite disappeared. Quartz and metallic iron also vanished and hematite (ferric iron) content decreased.

The corresponding Mössbauer spectrum (Fig. S3 in SM section) also shows four doublets denoting the presence of non-stoichiometric magnesiowüstite and a hfd associated to a minor contribution of other iron oxides. However, in this last case the iron distribution of non-equivalent sites in magnesiowustite was markedly different. It is worth to note the lower proportion of D3 sites (Table 3), evincing the leaching of Fe and Mn active species and suggesting that they are preferentially separated from the kind of site having more cation vacancies. The proportion associated to the hfd also diminished with respect to that in the EAFS spectrum. This is another proof of Fe leaching.

After conducting stability tests at both natural pH and pH 3, attrition of the catalyst was observed (see SM Figure S7). This phenomenon was a direct result of the ongoing abrasion that the catalyst particles experienced during each oxidation test. However, it is important to note that the reduction in particle size did not result in any discernible improvement in mineralization levels over the testing cycles.

Conclusions

A solid waste from the steel industry, EAFS, was tested as a catalyst for the ozonation of emerging pollutant, BPA. The sample was characterized thoroughly by several techniques, such as SEM/EDX, XRD, surface area, pH_{PZC} and Mössbauer spectroscopy. A low surface area, alkaline nature and a composition rich in Fe, Ca, Si, C oxides, with minor contents of Mg, Mn and Al were determined. The elements detected in the leachability test did not exceed the maximum admitted for sewage discharge in the Argentinian region.

The reactivity of BPA towards ozone was high in the explored experimental condition; the compound completely disappeared after 20 min of reaction independently of pH condition and ozonation process type (single or catalyzed). However, since reaction intermediates from BPA ozonation were refractory towards ozone attack, limited mineralization levels were achieved in the single ozonation experiments, especially at acidic conditions. TOC conversion was lower than 30 % for pH lower than 6. BPA mineralization could be enhanced up to 65% by increasing the pH to 10, due to the formation of active and non-selective HO• species favored by alkaline conditions.

EAFS improved the mineralization degree of BPA at acidic and alkaline conditions with respect to those achieved in single ozonation processes (Fig. 7). The high TOC conversion reached at alkaline pH (80 %) was due to the generation of HO• -promoted by OH^-- combined with precipitation reactions caused by Ca oxides. The outstanding improvement in the mineralization level at pH 3 (63 %) was attributed to the activity of leached species, mostly Fe and Mn cations.

At pH 3, the activity of EAFS is mostly sustained after 4 cycles (3 h each), this fact can be related to the large amount of available Fe. A reduction of activity was observed in experiments with no controlled pH conditions, which is linked to the loss of alkaline conditions. However, the residual activity still allowed BPA mineralization levels over 50 %.

EAFS showed very high activity and reasonable stability for the mineralization of BPA in catalytic ozonation process. The proposal offers an appealing alternative for the valorization of this industrial waste and for the development of a low-cost process for wastewater treatment.

Acknowledgements

Financial support from CONICET. UNMdP. ANPCyT (PICT 2021-00026 and PICT 2019-0935) (Argentina). Authors thank Prof. G. Zerjav and Prof. A. Pintar from National Institute of Chemistry, Ljubljana, Slovenia, for their collaboration in N_2 adsorption-desorption experiments.

References

[1] M. Petrović, S. Gonzalez, D. Barceló, Analysis and removal of emerging contaminants in wastewater and drinking water, Trends Anal. Chem. 22 (2003) 685–696.

[2] J.N. Hahladakis, E. Iacovidou, S. Gerassimidou, An overview of the occurrence, fate, and human risks of the bisphenol-A present in plastic materials, components, and products, Integr. Envir. Assess & Manag. 19 (2023) 45–62. https://doi.org/10.1002/ieam.4611.

[3] P.V.L. Reddy, K.-H. Kim, B. Kavitha, V. Kumar, N. Raza, S. Kalagara, Photocatalytic degradation of bisphenol A in aqueous media: A review, J. Environ. Manage. 213 (2018) 189–205. https://doi.org/10.1016/j.jenvman.2018.02.059.

[4] S.A. Mirzaee, N. Jaafarzadeh, S. Jorfi, H.T. Gomes, M. Ahmadi, Enhanced degradation of Bisphenol A from high saline polycarbonate plant wastewater using wet air oxidation, Process Saf. Environ. Prot. 120 (2018) 321–330. https://doi.org/10.1016/j.psep.2018.09.021.

[5] T. Yamamoto, A. Yasuhara, H. Shiraishi, O. Nakasugi, Bisphenol A in hazardous waste landfill leachates, Chemosphere. 42(4) (2001) 415-8. doi: 10.1016/s0045-6535(00)00079-5. PMID: 11100793.

[6] J.-H. Kang, D. Aasi, Y. Katayama, Bisphenol A in the aquatic environment and its endocrine-disruptive effects on aquatic organisms, Crit. Rev. Toxicol. 37 (2007) 607–625. https://doi.org/10.1080/10408440701493103.

[7] C. von Sonntag, U. von Gunten, Chemistry of ozone in water and wastewater treatment: From basic principles to applications, IWA Publishing, 2012. https://doi.org/10.2166/9781780400839.

[8] T. Garoma, S.A. Matsumoto, Y. Wu, R. Klinger, Removal of Bisphenol A and its reaction-intermediates from aqueous solution by ozonation, Ozone: Sci. Eng. 32 (2010) 338–343. https://doi.org/10.1080/01919512.2010.508484.

[9] M. Deborde, S. Rabouan, J.-P. Duguet, B. Legube, Kinetics of aqueous ozone-induced oxidation of some endocrine disruptors, Environ. Sci. Technol. 39 (2005) 6086–6092. https://doi.org/10.1021/es0501619.

[10] J.N. Sahu, Y. Kapelyushin, D.P. Mishra, P. Ghosh, B.K. Sahoo, E. Trofimov, B.C. Meikap, Utilization of ferrous slags as coagulants, filters, adsorbents, neutralizers/stabilizers, catalysts, additives, and bed materials for water and wastewater treatment: A review, Chemosphere. 325 (2023) 138201. https://doi.org/10.1016/j.chemosphere.2023.138201.

[11] V. Matthaiou, P. Oulego, Z. Frontistis, S. Collado, D. Hela, I.K. Konstantinou, M. Diaz, D. Mantzavinos, Valorization of steel slag towards a Fenton-like catalyst for the degradation of paraben by activated persulfate, Chem. Eng. J. 360 (2019) 728–739. https://doi.org/10.1016/j.cej.2018.11.198.

[12] N. Nasuha, S. Ismail, B.H. Hameed, Activated electric arc furnace slag as an efficient and reusable heterogeneous Fenton-like catalyst for the degradation of Reactive Black 5, J. Taiwan Inst. Chem. Eng. 67 (2016) 235–243. https://doi.org/10.1016/j.jtice.2016.07.023.

[13] N. Nasuha, S. Ismail, B.H. Hameed, Activated electric arc furnace slag as an effective and reusable Fenton-like catalyst for the photodegradation of methylene blue and acid blue 29, J. Environ. Manage. 196 (2017) 323–329. https://doi.org/10.1016/j.jenvman.2017.02.070.

[14] N. Nasuha, B.H. Hameed, P.U. Okoye, Dark-Fenton oxidative degradation of methylene blue and acid blue 29 dyes using sulfuric acid-activated slag of the steel-making process, J. Environ. Chem. Eng. 9 (2021) 104831. https://doi.org/10.1016/j.jece.2020.104831.

[15] R. Mecozzi, L. Di Palma, D. Pilone, L. Cerboni, Use of EAF dust as heterogeneous catalyst in Fenton oxidation of PCP contaminated wastewaters, J. Hazard. Mater. 137 (2006) 886–892. https://doi.org/10.1016/j.jhazmat.2006.03.002.

[16] H.T. Van, L.H. Nguyen, T.K. Hoang, T.P. Tran, A.T. Vo, T.T. Pham, X.C. Nguyen, Using FeO-constituted iron slag wastes as heterogeneous catalyst for Fenton and ozonation processes to degrade Reactive Red 24 from aqueous solution, Sep. Purif. Technol. 224 (2019) 431–442. https://doi.org/10.1016/j.seppur.2019.05.048.

[17] N.T. Hien, L.H. Nguyen, H.T. Van, T.D. Nguyen, T.H.V. Nguyen, T.H.H. Chu, T.V. Nguyen, V.T. Trinh, X.H. Vu, K.H.H. Aziz, Heterogeneous catalyst ozonation of Direct Black 22 from aqueous solution in the

presence of metal slags originating from industrial solid wastes, Sep. Purif. Technol. 233 (2020) 115961. https://doi.org/10.1016/j.seppur.2019.115961.

[18] T. Preoanin, N. Kallay, Application of »Mass Titration« to Determination of Surface Charge of Metal Oxides, Croat. Chem. Acta. 71 (1998) 1117–1125.

[19] R. Baird, L. Bridgewater, Standard methods for the examination of water and wastewater. 23rd edition. Washington, D.C., 2017, American Public Health Association.

[20] B. Kasprzyk-Hordern, M. Ziółek, J. Nawrocki, Catalytic ozonation and methods of enhancing molecular ozone reactions in water treatment, Appl. Catal. B. 46 (2003) 639–669. https://doi.org/10.1016/S0926-3373(03)00326-6.

[21] G.R. Qian, D.D. Sun, J.H. Tay, Z.Y. Lai, Hydrothermal reaction and autoclave stability of Mg bearing RO phase in steel slag, Br. Ceram. Trans. 101 (2002) 159–164. https://doi.org/10.1179/096797802225003415.

[22] I. Strandkvist, Å. Sandström, F. Engström, Effect of FeO/MgO ratio on dissolution and leaching of magnesiowüstite, Steel Res. Int. 88 (2017) 1600322. https://doi.org/10.1002/srin.201600322.

[23] Bataleva, Palyanov, Borzdov, Bayukov, Processes and conditions of the origin for Fe^{3+}-bearing magnesiowüstite under lithospheric mantle pressures and temperatures, Minerals. 9 (2019) 474. https://doi.org/10.3390/min9080474.

[24] M. Ahmaruzzaman, Industrial wastes as low-cost potential adsorbents for the treatment of wastewater laden with heavy metals, Adv. Colloid Interface Sci. 166 (2011) 36–59. https://doi.org/10.1016/j.cis.2011.04.005.

[25] S.K. Singh, P. Vashistha, R. Chandra, A.K. Rai, Study on leaching of electric arc furnace (EAF) slag for its sustainable applications as construction material, Process Saf. Environ. Prot. 148 (2021) 1315–1326. https://doi.org/10.1016/j.psep.2021.01.039.

[26] I. Gultekin, V. Mavrov, N.H. Ince, Degradation of bisphenol-A by ozonation, J. Adv. Oxid. Technol. 12 (2009). https://doi.org/10.1515/jaots-2009-0215.

[27] L. Zhou, S. Wang, Z. Li, X. Cao, R. Liu, J. Yun, Simultaneously removal of phosphorous and COD for purification of organophosphorus wastewater by catalytic ozonation over CaO, J. Water Process Eng. 51 (2023) 103397. https://doi.org/10.1016/j.jwpe.2022.103397.

[28] M. Izadifard, G. Achari, C.H. Langford, Mineralization of sulfolane in aqueous solutions by Ozone/CaO_2 and Ozone/CaO with potential for field application, Chemosphere. 197 (2018) 535–540. https://doi.org/10.1016/j.chemosphere.2018.01.072.

[29] X. Quan, D. Luo, J. Wu, R. Li, W. Cheng, shuping Ge, Ozonation of acid red 18 wastewater using O_3/$Ca(OH)_2$ system in a micro bubble gas-liquid reactor, J. Environ. Chem. Eng. 5 (2017) 283–291. https://doi.org/10.1016/j.jece.2016.12.007.

[30] J. Chen, Y. Tu, G. Shao, F. Zhang, Z. Zhou, S. Tian, Z. Ren, Catalytic ozonation performance of calcium-loaded catalyst (Ca-C/Al_2O_3) for effective treatment of high salt organic wastewater, Sep. Purif. Technol. 301 (2022) 121937. https://doi.org/10.1016/j.seppur.2022.121937.

[31] F. Firdiyono, L.H. Lalasari, E. Tarmizi, E. Sulistiyono, L. Andriyah, T. Arini, N.C. Natasha, F.E. Yunita, The degree of lithium (Li) stability compared to calcium (Ca) and magnesium (Mg) from low lithium grade brine water with addition of limestone and oxalic Acid, IOP Conf. Ser.: Mater. Sci. Eng. 858 (2020) 012044. https://doi.org/10.1088/1757-899X/858/1/012044.

[32] X. Huang, F. Yan, R. Guo, H. He, H. Li, Study of steel slag eroded by oxalic acid and recovery of leachate, Sustainability. 14 (2022) 13598. https://doi.org/10.3390/su142013598.

[33] W. Chen, X. Li, Z. Pan, S. Ma, L. Li, Effective mineralization of Diclofenac by catalytic ozonation using Fe-MCM-41 catalyst, Chem. Eng. J. 304 (2016) 594–601. https://doi.org/10.1016/j.cej.2016.06.139.

[34] F. Qi, B. Xu, Z. Chen, L. Zhang, P. Zhang, D. Sun, Mechanism investigation of catalyzed ozonation of 2-methylisoborneol in drinking water over aluminum (hydroxyl) oxides: Role of surface hydroxyl group, Chem. Eng. J. 165 (2010) 490–499. https://doi.org/10.1016/j.cej.2010.09.047.

[35] S. Larouk, R. Ouargli, D. Shahidi, L. Olhund, T.C. Shiao, N. Chergui, T. Sehili, R. Roy, A. Azzouz, Catalytic ozonation of Orange-G through highly interactive contributions of hematite and SBA-16 – To better understand azo-dye oxidation in nature, Chemosphere. 168 (2017) 1648–1657. https://doi.org/10.1016/j.chemosphere.2016.11.120.

[36] H. Yan, W. Chen, G. Liao, X. Li, S. Ma, L. Li, Activity assessment of direct synthesized Fe-SBA-15 for catalytic ozonation of oxalic acid, Sep. Purif. Technol. 159 (2016) 1–6. https://doi.org/10.1016/j.seppur.2015.12.055.

[37] Y. Dong, K. He, B. Zhao, Y. Yin, L. Yin, A. Zhang, Catalytic ozonation of azo dye active brilliant red X-3B in water with natural mineral brucite, Catal. Commun. 8 (2007) 1599–1603. https://doi.org/10.1016/j.catcom.2007.01.016.
[38] K. He, Y.M. Dong, Z. Li, L. Yin, A.M. Zhang, Y.C. Zheng, Catalytic ozonation of phenol in water with natural brucite and magnesia, J. Hazard. Mater. 159 (2008) 587–592. https://doi.org/10.1016/j.jhazmat.2008.02.061.
[39] Y. Guo, H. Wang, B. Wang, S. Deng, J. Huang, G. Yu, Y. Wang, Prediction of micropollutant abatement during homogeneous catalytic ozonation by a chemical kinetic model, Water Res. 142 (2018) 383–395. https://doi.org/10.1016/j.watres.2018.06.019.
[40] N. Inchaurrondo, C. di Luca, G. Žerjav, J.M. Grau, A. Pintar, P. Haure, Catalytic ozonation of an azo-dye using a natural aluminosilicate, Catal. Today. 361 (2021) 24–29. https://doi.org/10.1016/j.cattod.2019.12.019.
[41] W. Yang, B. Vogler, Y. Lei, T. Wu, Metallic ion leaching from heterogeneous catalysts: an overlooked effect in the study of catalytic ozonation processes, Environ. Sci.: Water Res. Technol. 3 (2017) 1143–1151. https://doi.org/10.1039/C7EW00273D.
[42] R. Andreozzi, A. Insola, V. Caprio, R. Marotta, V. Tufano, The use of manganese dioxide as a heterogeneous catalyst for oxalic acid ozonation in aqueous solution, Appl. Catal. A: Gen. 138 (1996) 75–81. https://doi.org/10.1016/0926-860X(95)00247-2.
[43] J. Ma, N.J.D. Graham, Degradation of atrazine by manganese-catalysed ozonation—influence of radical scavengers, Wat. Res. 34 (2000) 3822-3828. https://doi.org/10.1016/S0043-1354(00)00130-5.
[44] D. Gregory, K.H. Carlson, Ozonation of dissolved manganese in the presence of natural organic matter, Ozone: Sci. Eng. 23 (2001) 149–159. https://doi.org/10.1080/01919510108961997.

Tables

Table 1. Experimental reaction conditions and tests designations for ozonation and complementary experiments.

Test	Experiment designation	Initial pH	Experiment details
# 1	O_3 – 10	10	Single ozonation at alkaline condition. Initial pH adjusted by adding NaOH.
# 2	O_3 – 3	3	Single ozonation at acidic condition. Initial pH adjusted by adding HNO_3.
# 3	O_3 – EAFS – 10	10.5	Catalytic ozonation with EAFS particles at alkaline condition. Initial pH was the natural alkaline one (10.5) and shifted to 9.5 at the end of test (mean pH=10)
# 4	O_3 – EAFS – 3	3	Catalytic ozonation with EAFS particles at acidic condition. Initial pH adjusted by adding HNO_3.
# 5	O_3 – Supernatant – 10	10.5	Catalytic ozonation with supernatant prepared at natural alkaline condition (pH=10.5). pH shifted to 8 at the end of the test (mean pH=9.25).
# 6	O_3 – Supernatant – 3	3	Catalytic ozonation using supernatant prepared at acidic condition (pH=3). pH kept acidic during the test.
# 7	O_3 – Fe – 3	3	Catalytic ozonation with Fe (III) salt (4.5 mg/L) at acidic condition.
# 8	O_3 – Mn – 3	3	Catalytic ozonation with Mn (II) salt (0.1 mg/L) at acidic condition.
# 9	O_3 – EAFS – 10 – (i)	10.5	EAFS reusage test at natural alkaline condition. (i) indicates the cycle number. pH gradually decreased

			with cycle number achieving pH=5.6 at the end of the 4th cycle.
# 10	O_3 – EAFS – 3 – (i)	3	EAFS reusage test at acidic condition. The number in parenthesis indicates the cycle number. pH kept acidic (pH=3) along the experiments.
# 11	O_3 – 6	7	Single ozonation at neutral condition. pH adjusted by adding HNO_3 along the test. pH varied between 7 and 5.5 (mean pH=6).
# 12	O_3 – 4	7	Single ozonation at initial neutral condition. pH was not adjusted. pH varied between 7 and 3.9 (mean pH=4.2).
# 13	O_3 – 5.5	6	Single ozonation at slightly acidic condition. pH adjusted by adding HNO_3 along the test. pH varied between 6 and 5 (mean pH=5.4).
# 14	O_3 – 8	9	Single ozonation at slightly basic condition. pH adjusted by adding NaOH along the test. pH varied between 9 and 7 (mean pH=8).
# 15	Ads -10	10	Adsorption (20 mg/L BPA- 0,5 g/L EAFS at pH 10)
# 16	Ads -3	3	Adsorption (20 mg/L BPA- 0,5 g/L EAFS at pH 3)
# 17	O_3 – EAFS- Ads – 10	10.5	Single ozonation test at pH 10 followed by EAFS adsorption test at natural alkaline condition.

Table 2. EDS composition of raw EAFS and reused EAFS samples.

Element	**EAFS Raw sample**	**EAFS sample O_3 – EAFS – 10 – (4)**	**EAFS sample O_3 – EAFS – 3 – (4)**
O	41.1 ± 7.6	36.4 ± 12.4	38.6 ± 4.1
Fe	16.2 ± 2.4	31.7 ± 12.6	34.2 ± 5.7
Ca	13.2 ± 1.9	7.9 ± 3.8	1 ± 0
C	18.9 ± 9.2	12.8 ± 3.9	10.5 ± 1.4
Si	3.7 ± 0.5	1.3 ± 0.5	2.9 ± 1.9
Mg	2.6 ± 0.4	3.6 ± 1.0	6.7 ± 1.2
Mn	1.8 ± 0.5	3.0 ± 0.9	3.9 ± 0.6
Al	1.4 ± 0.2	1.5 ± 0.4	0.7 ± 0.3
Cr	0.6 ± 0.1	1.3 ± 0.8	0.5 ± 0.3
Ti	0.2 ± 0.1	0.5 ± 0.2	0.1 ± 0.1
Cu	0.1 ± 0.1	0.1 ± 0.2	0.1 ± 0.1

Table 3. Mössbauer hyperfine parameters and relative proportion of sites (%) in magnesiowustite and of the hfd comprising other minor iron oxides, oxyhydroxide and metallic iron for the raw slag sample (EAFS), and for those samples after 4 cycles reusing at initial pH 10 (without pH control) and at pH 3. QS: quadrupole splitting, Bhf: mean hyperfine field of the distribution.

Sample	**Parameters**	**hfd**	**D1**	**D2**	**D3**	**D4**
EAFS	IS [mm/s]	0.42	1.03	1.04	1.05	0.38
	QS [mm/s]	-	0.75	1.17	1.71	0.87

	Bhf [T]	42.0	-	-	-	-
	%	18	29	24	18	11
4 cycles pH 10	IS [mm/s]	0.52	1.04	1.03	1.06	0.39
	QS [mm/s]	-	0.71	1.07	1.58	0.79
	Bhf [T]	39.5	-	-	-	-
	%	19	21	24	24	14
4 cycles pH 3	IS [mm/s]	0.22	1.04	1.03	1.08	0.36
	QS [mm/s]	-	0.86	1.41	1.95	0.86
	Bhf [T]	41.0	-	-	-	-
	%	10	46	27	6	11

Table 4. Leached Fe and Mn cations and initial and final pH measured over the ozonation cycles in EAFS stability tests (#9 and #10 -Table 1).

	Cycles without pH control O_3 -EFAS-10-(i)				**Cycles at acidic conditions O_3 -EFAS-3-(i)**			
(i)	***1***	***2***	***3***	***4***	***1***	***2***	***3***	***4***
Initial pH	10.5	9.2	7	7	3	3	3	3
Final pH	9.5	8.5	6.7	5.6	3	3	3	3
Leached Fe ions (mg/L)	0	0.20	0.13	0.40	6.41	3.73	4.18	3.47
Leached Mn ions (mg/L)	0	0.10	0.06	0.12	0.41	0.06	0.08	0.08

Figures

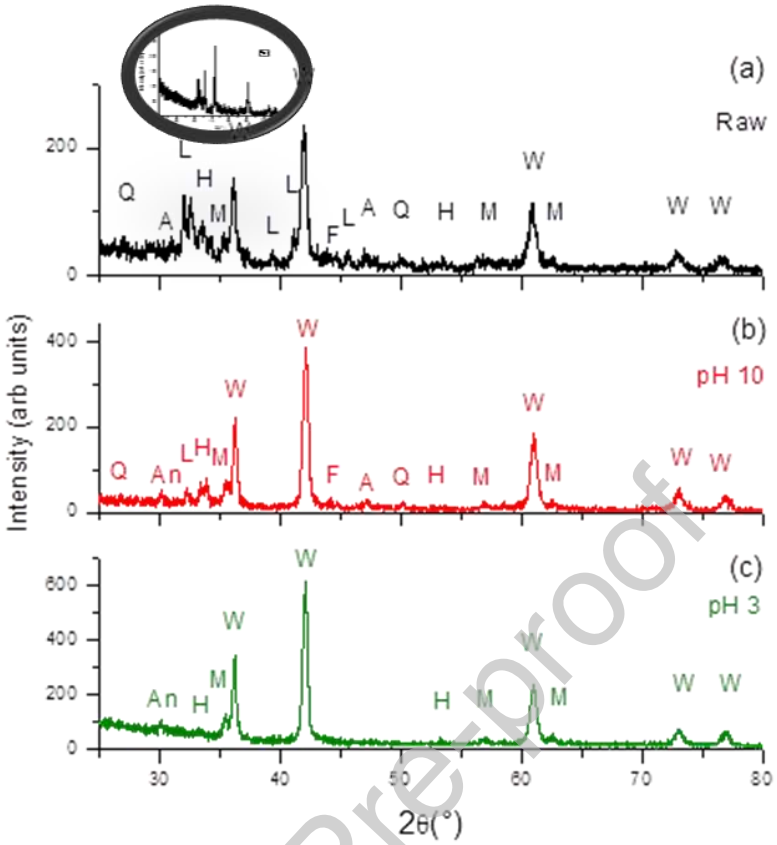

Figure 1. XRD diffractogram of the raw slag sample (upper panel) and of the 4 cycles reused samples (lower panels). Insert: view of the low diffraction angles. The main peaks of each compound are identified: W - wustite, L - larnite, H - hematite, M - magnetite/maghemite, Q - quartz, An - ankerite, A - akermanite, F - metallic iron.

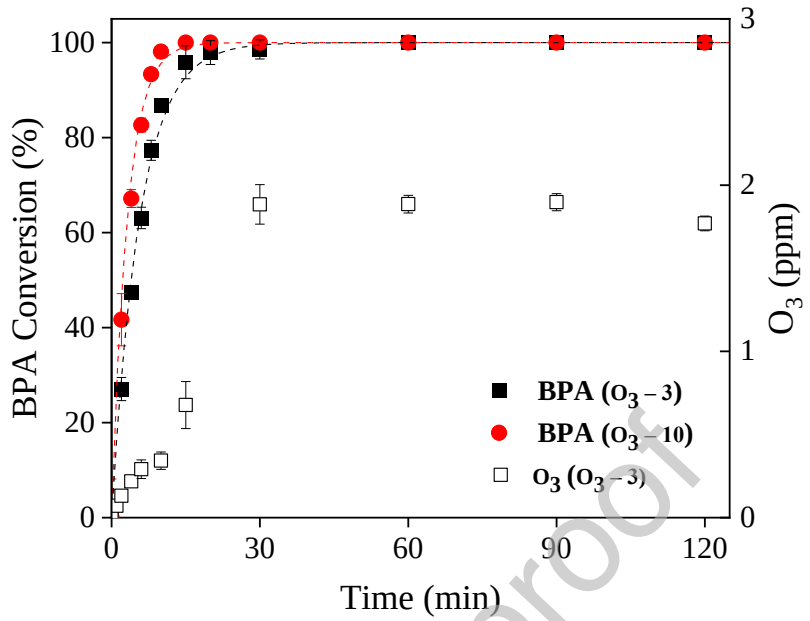

Figure 2. Evolution of BPA conversion and O_3 aqueous concentration during single ozonation experiments (tests #1 and #2, Table 1). The dash lines show the pseudo-1st order reaction rate fittings (regression coefficients are 0.9961 and 0.9928 for O_3-3 and O_3-10, respectively).

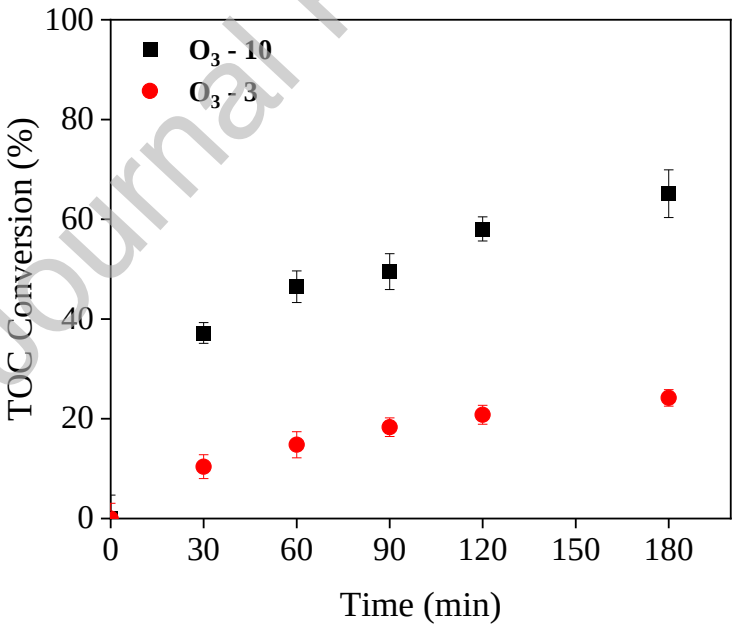

Figure 3. TOC conversion evolution during single ozonation experiments (tests #1 and #2, Table 1).

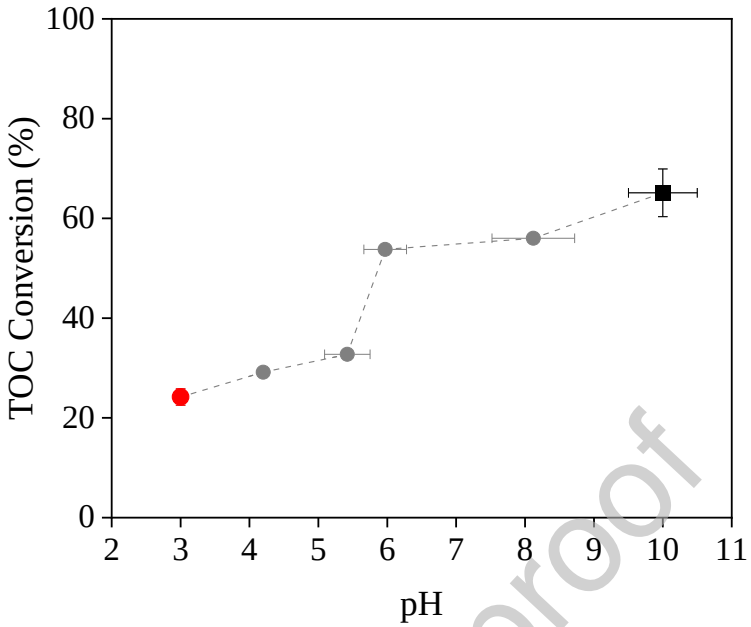

Figure 4. TOC conversion achieved in single ozonation experiments at different pH conditions after 3 h of reaction. Data registered at the end of tests #1, #2, #11, #12, #13 and #14 (Table 1).

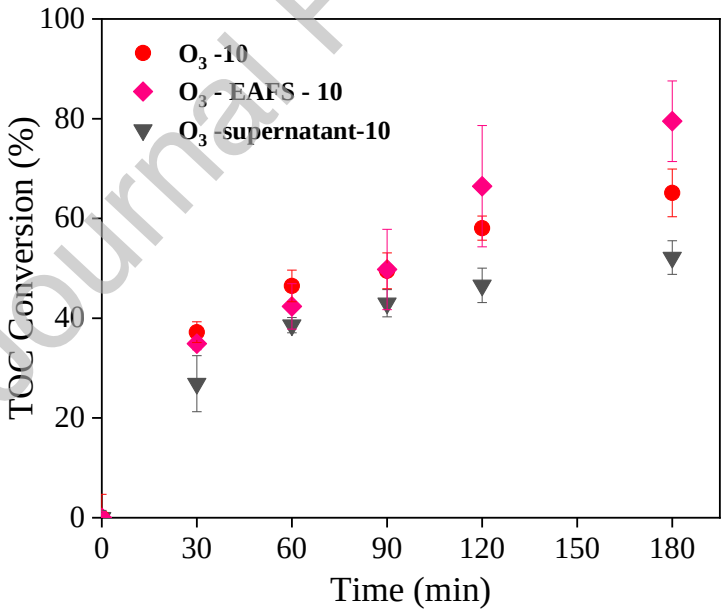

a)

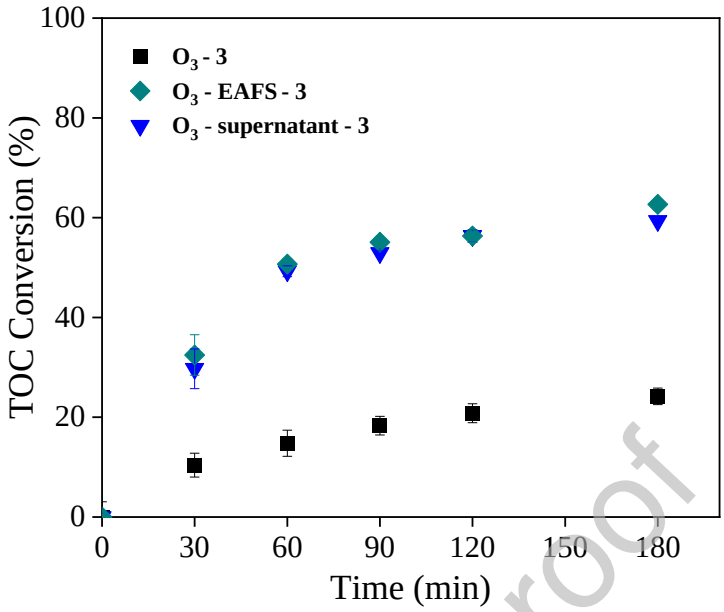

b)

Figure 5. TOC conversion evolution during ozonation experiments at different pH conditions: ***a)*** alkaline (tests #1, #3 and #5, Table 1); ***b)*** acidic (#2, #4 and #6, Table 1).

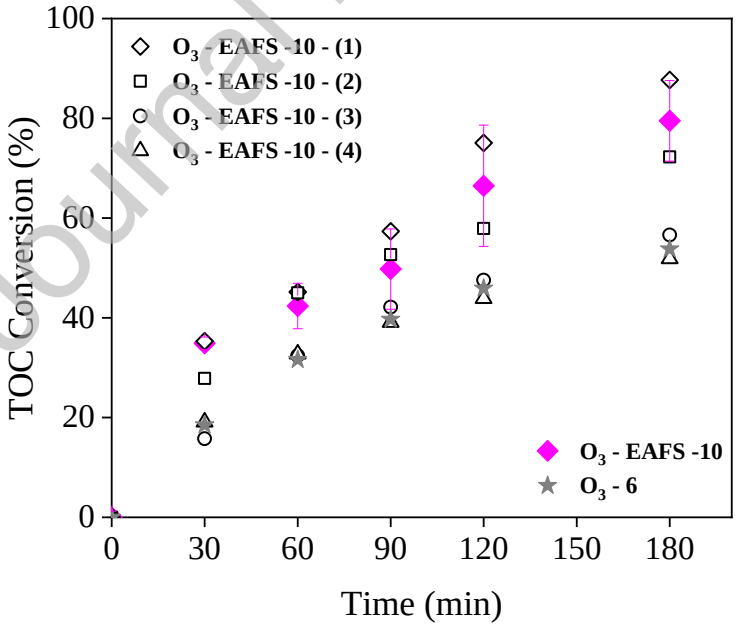

a)

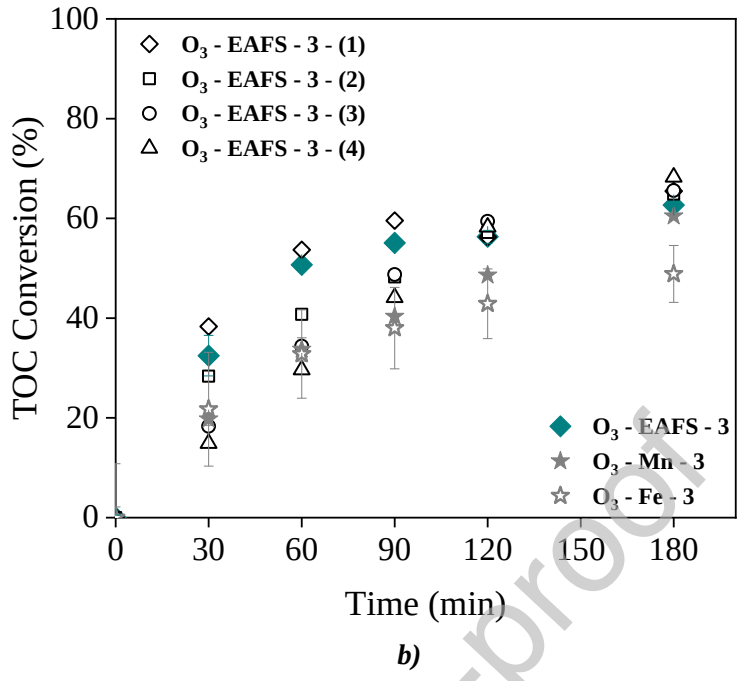

b)

Figure 6. TOC conversion evolution during ozonation experiments for EAFS stability studies at different pH conditions: ***a***) uncontrolled (test # 9, Table 1); ***b***) acidic (test #10, Table 1). Complementary ozonation tests results (# 11 -Table 1) and (test # 7 and # 8, Table 1) are included for comparison.

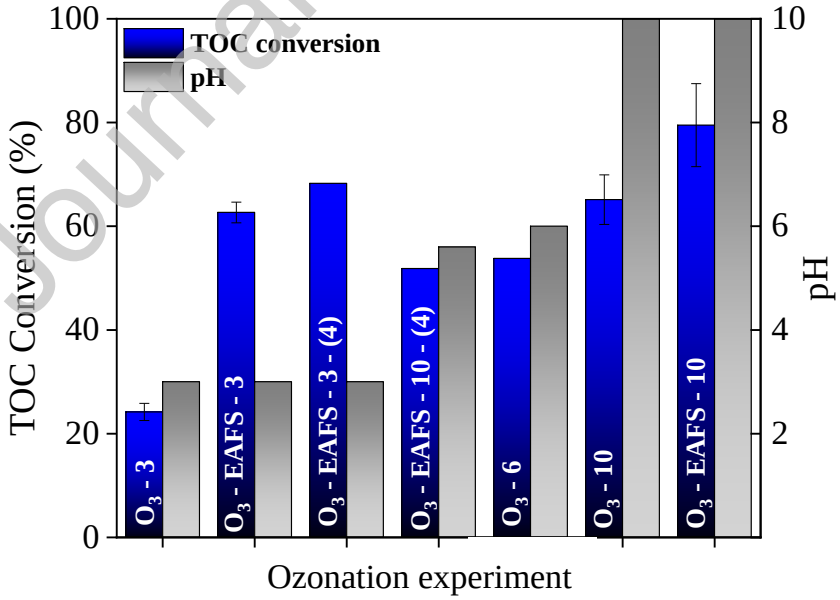

Figure 7. Mean pH and TOC conversion achieved under several ozonation conditions after 3 h of reaction.

Financial support from:

- CONICET.
- UNMdP.
- ANPCyT (PICT 2021-00026 and PICT 2019-0935) (Argentina).

Declaration of interests

☒ The authors declare that they have no known competing financial interests or personal relationships that could have appeared to influence the work reported in this paper.

☐The authors declare the following financial interests/personal relationships which may be considered as potential competing interests: